ORIGINAL ARTICLE

Ultra Performance Liquid Chromatography-High-Resolution Mass Spectrometry Profiling and Molecular Dynamics Reveals *Ammannia baccifera* as a Modulator of the Keap1-Nrf2 Signaling Pathway

Nemalapalli Yamini[1], Juturu Mastanaiah[2]

[1]Department of Pharmacology, JNTUA-OTPRI, Jawaharlal Nehru Technological University, Anantapur, Andhra Pradesh, India, [2]Department of Pharmacology, Balaji College of Pharmacy, Anantapur, Andhra Pradesh, India

Abstract

Cardiovascular disease (CVDs) is a major cause of death worldwide. The present study investigated the cardioprotective potential of *Ammannia baccifera* against the Keap1–Nrf2 signaling pathway using a multilevel *in silico* strategy. The bioactive compounds of *A. baccifera* were profiled using liquid chromatography-high-resolution mass spectrometry analysis and screened by molecular docking against the Keap1 Kelch domain (PDB: 4L7D). The study revealed that some biologically active ligands, such as (3R)-4′-Methoxy-2′,3,7-trihydroxyisoflavanone (−7.024 kcal/moL), 6,7,4′-Trihydroxyisoflavanone (−6.713 kcal/moL), cyanidin 3-O-sambubioside (−6.644 kcal/moL), 2′,7-Dihydroxy-4′,5′-dimethoxyisoflavone (−6.416 kcal/moL), Irilone (−6.503 kcal/moL), and Astilbin (−6.175 kcal/moL) exhibited good docking scores and high binding free energies, establishing stable hydrogen bonds with important residues, such as THR41, ARG35, and SER32, which provided a combination of hydrogen bonds and hydrophobic contacts to the ligand along the trajectory, which are reported to regulate Nrf2 ubiquitination. These compounds predominantly belong to the isoflavonoid, flavonoid glycoside, and anthocyanin classes, which are rich in hydrogen bonding potential and planar aromatic rings, which may enable strong π-π stacking and van der Waals interactions within the active site. Furthermore, molecular dynamics simulations for >200 ns confirmed the structural stability, persistent hydrogen bonding, and long-term duration of these interactions with active compounds. The important ligands exhibited stable paths and low root mean square fluctuation, confirming their binding stability under physiological conditions. In addition, absorption, distribution, metabolism, excretion, and toxicity, and Lipinski profiling showed good oral bioavailability, negligible cardiotoxicity (human ether-a-go-go-related gene inhibition risk), high passive permeability, and tolerable solubility for the selected compounds. The potential antioxidant effects of *A. baccifera* (2, 2'-azino-bis [3-ethylbenzothiazoline-6-sulphonic acid] and ferric reducing antioxidant power assays) and free radical scavenging effects (2-Diphenyl-1-Picrylhydrazyl assay) further confirmed its potential to modulate the Keap1-Nrf2 signaling pathway. This study concludes that *A. baccifera* may be a potential lead source for developing next-generation drugs targeting the Keap1-Nrf2 signaling pathway in CVDs.

Key words: *Ammannia baccifera,* antioxidant, cardio protection, Keap1-Nrf2 pathway, molecular docking

INTRODUCTION

Ischemic heart disease remains the major cause of cardiovascular morbidity and mortality worldwide.[1] Blockage of coronary blood flow results in acute coronary syndrome through oxygen deficiency in cardiomyocytes, leading to a disruption in oxidative phosphorylation and adenosine triphosphate

Address for correspondence:
Juturu Mastanaiah, Department of Pharmacology, Balaji College of Pharmacy, Anantapur, Andhra Pradesh, India.
E-mail: masthpharma@gmail.com

Received: 19-05-2026
Revised: 22-06-2026
Accepted: 29-06-2026

synthesis. Consequently, metabolic dysregulation, ionic imbalances, inflammation, and apoptosis occur. However, despite the importance of re-establishing coronary blood flow to preserve viable myocardial tissues, the reperfusion itself increases myocardial damage via oxidative stress, calcium accumulation, endothelial dysfunction, and inflammatory responses, referred to as ischemia-reperfusion injury.[2]

While present treatments, including pharmacological intervention and reperfusion techniques, have decreased mortality from ischemic attacks, cardiomyocyte damage and eventual heart failure due to ischemia-reperfusion injury still pose considerable problems. This calls for further methods for the protection of the heart, which would prevent damage to cardiac cells and thus help maintain their functions during the reperfusion process. The dysfunction of mitochondria in ischemia-reperfusion injury is caused by electron transport chain malfunction, Reactive oxygen species (ROS) overload, opening of mitochondrial permeability transition pore (mPTP), and mitochondrial dynamics disruption.[3] In recent years, bioactive natural product compounds have gained significant attention in modern therapeutic systems, particularly for their potential role in preventing cardiac disorders through their powerful antioxidative mechanisms, such as scavenging ROS.[4] Herbal drugs are still an essential part of healthcare worldwide and remain deeply integrated into the traditional ways of many cultures. The most frequently valued compounds in this respect are polyphenolic phytochemicals, which exert their cardioprotective effects mainly by preventing LDL oxidation, an important step in the development of atherosclerosis.[5] A substantial proportion of clinically important drugs originate from plants, highlighting the pivotal contribution of plant-derived compounds to both human and veterinary medicine. These natural agents are used not only for the management of diverse pathological conditions but also to maintain overall physiological well-being. Medicinal plants have been widely used for centuries to prevent and treat ischemic heart diseases, and over the past decades, accumulating phytochemical, pharmacological, and clinical evidence has increased the relevance of plant-based therapeutics in contemporary healthcare.[6]

A number of medicinal plants, such as *Daucus carota*, *Nerium oleander*, *Ginkgo biloba*, *Terminalia arjuna*, *Tinospora cordifolia*, and *Mucuna pruriens,* have shown promising cardioprotective effects in laboratory and clinical trials. They are abundant in various phytochemicals with medical importance. Out of these, *Ammannia baccifera* L. (Lythraceae), growing in the paddy fields of India, has been used in Ayurveda for its cathartic, stomachic, hepatoprotective, and aphrodisiac effects.[7] In Unani medicine, they are used to stimulate appetite and treat rheumatic pains and fever, while in Siddha medicine, the plant as a whole is used to treat glandular swellings, leukorrhea, snakebite poisoning, abscesses, ulcers, and polyuria. The major phytochemical constituent of its leaves has been identified to be lawsone. It exhibits anti-typhoid, anti-tubercular, anti-tumor, and extensive antimicrobial activities against human and plant pathogenic fungi.[8,9] Other flavonoids present in *Ammannia* spp. include quercetin, rutin, luteolin, isorhamnetin, apigenin, vitexin, kaempferol derivatives, rhamnetin, and its glycosides. In this study, we performed comprehensive metabolite profiling of the methanolic extract of *A. baccifera* L. using liquid chromatography-high-resolution mass spectrometry (LC-HRMS), followed by computational analyses of the identified metabolites to evaluate their potential cardioprotective properties.

MATERIALS AND METHODS

Materials

Chemicals

All chemicals and solvents used were of analytical grade.2, 2-Diphenyl-1-Picrylhydrazyl (DPPH), potassium ferricyanide, ferric chloride, butylated hydroxytoluene (BHT), and L-ascorbic acid were purchased from Merck Co., India. Glass-distilled water was used to prepare all reagents and solutions.

Sample collection and preparation of extracts

The aerial parts of *A. baccifera* were collected from local areas of Tirupathi district, Andhra Pradesh, India, authenticated, and deposited in the Botany Herbarium, Sri Venkateswara University (0397). The plant material was shade-dried, powdered, and used for ethanolic extraction.

Preparation of extract

The plant material was thoroughly washed with water, chopped into small pieces, and dried under sunlight until completely moisture-free. The dried material was then finely ground and subjected to successive extraction in a maceration process. The solvents from the resulting extracts were removed and the concentrated extracts were used for further experimental analyses.[10,11]

High-resolution liquid chromatography and mass spectrometry (HR-LCMS)

In this study, ultra-high-performance liquid chromatography coupled with tandem high-resolution mass spectrometry (UHPLC-HRMS) was used to identify the bioactive constituents in the ethanolic fraction of *A. baccifera*. The fraction was analyzed using an Agilent 1260 Infinity II UHPLC system coupled to an Agilent 6540 quadrupole time-of-flight (Q-TOF) mass spectrometer fitted with a column compartment, Hip sampler, Agilent Dual ESI source, and a binary pump for chromatographic separation. A 5 µL aliquot of the sample was injected onto an ACQUITY UPLC HSS T3 column (100 mm × 2.1 mm, 1.8 µm) maintained at 20°C. Separation was performed using a gradient elution system consisting of 0.1% formic acid in water (solvent A) and acetonitrile (solvent B) at a flow rate of 0.2 mL/min.

The gradient program started from 95% A and 5% B, then linearly changed to 5% A and 95% B in 25 min, maintained for 5 min, then returned to its starting composition within 2 min, followed by an 8-min re-equilibration period. Mass spectrometric detection was performed in both positive and negative electrospray ionization modes. The scan range was set at m/z 50–2000, with a resolving power of 30,000–60,000, spray voltage of 4.5 kV, sheath gas of 12 arbitrary units, auxiliary gas of 10 arbitrary units, and capillary temperature of 350°C.

Anti-oxidant activity

DPPH radical quenching capacity

The DPPH assay was used to determine the free radical scavenging potential of the extracts according to the procedure described by Singleton VL *et al*., Various concentrations (10–1000 µg/mL) of the extracts were combined with 0.1 mM of DPPH methanol solution, vigorously shaken, and allowed to stand in darkness for 20 min at 25°C. The absorbance readings were taken at 517 nm using a Shimadzu UV-2401PC ultraviolet-visible (UV-Vis) Spectrophotometer, while methanolic DPPH was used as the control sample, and methanol was the blank sample. The antioxidant activity was calculated in terms of 50% inhibitory concentration (IC_{50}) values. Ascorbic acid, as well as BHT, served as standards.[12]

The percentage quenching of DPPH was calculated as follows:

$$\text{DPPH• quenching capacity } (\%) = \frac{(\text{Abs}_{\text{control}}) - (\text{Abs}_{\text{sample}})}{\text{Abs}_{\text{control}}} \times 100 \quad (1)$$

$$\text{DPPH quenching capacity } (\%) = (\text{Abs}_{\text{control}}) - (\text{Abs}_{\text{sample}})$$

Where, $\text{Abs}_{\text{sample}}$ is absorbance of the sample (extract and standard antioxidant) and $\text{Abs}_{\text{control}}$ is the DPPH solution without the added extract.

Ferric reducing-antioxidant capacity

The reducing power of the extracts was investigated using the potassium ferricyanide reduction assay adapted from Oyaizu. Briefly, various concentrations (10–1000 µg/mL) of each extract were mixed with sodium phosphate buffer (0.2 M, pH 6.6) and 1% potassium ferricyanide, followed by incubation at 50°C for 20 min. After the addition of 10% trichloroacetic acid and centrifugation, the supernatant was mixed with deionized water and 1% $FeCl_3$ solution and incubated at 35°C for 10 min for Prussian blue complex formation. Absorbance was measured at 700 nm using a Shimadzu UV-2401PC UV-Vis spectrophotometer, where higher absorbance indicated greater reducing power, with ascorbic acid and BHT used as reference standards.[6]

In vitro 2, 2'-azino-bis (3-ethylbenzothiazoline-6-sulphonic acid) ($ABTS^+$) radical ion scavenging assay

The $ABTS^+$ radical ion scavenging assay was conducted as previously described, with slight adjustments (Hussen and Endalew, 2023).The reaction between 7 mM ABTS and 2.45 mM potassium persulfate resulted in the formation of the $ABTS^+$ radical cation solution by incubating it for 16 h under dark conditions. Next, 2 µL of the extract was added to 3 mL of $ABTS^+$ radical cation solution and allowed to react for 6 min before the absorbance was read at 734 nm. The results were presented as IC_{50} and expressed in mg gallic acid equivalent per gram of extract.

Statistical analysis of data

The statistical analysis was done with Statistical Package for the Social Sciences (SPSS) software (version 16.0) from SPSS Inc. (Chicago, IL, USA). The IC_{50} was determined by means of linear regression analysis, while Pearson correlation analysis was used to find out the correlation between total phenolics and antioxidant activity. Mean differences were tested for significance by applying the least significant difference test, where $P < 0.05$ was considered significant.

Computational studies

Molecular docking studies

Molecular docking studies were conducted for the identified metabolites against key protein targets involved in cardioprotective mechanisms. Accordingly, Kelch-like ECH-associated protein 1, lipid kinase phosphoinositide 3-kinase, transforming growth factor-beta receptor, and sirtuin 1 were selected as the receptor proteins. The intramolecular interactions of each complex were assessed in terms of binding affinity and stability. Docking simulations were performed using the Schrödinger Maestro Suite (version 2022), and the compounds were ranked according to their docking scores and calculated binding energies (kcal/mol).[13,14]

Molecular dynamics

These complexes between proteins and ligands were then simulated for 100 ns through the Desmond Molecular Dynamics program. These simulations were run after relaxing and equilibrating the systems based on certain criteria, such as Constant Number of particles, Volume, and Temperature (NVT) and Constant Number of particles, Pressure, and Temperature (NPT) equilibration steps. Simulations were done in NPT conditions at 300 K temperature and 1.01325 bar pressure, while taking frames at 1000 ps intervals.[15,16]

Absorption, distribution, metabolism, excretion, and toxicity (ADMET) analysis

The compounds exhibiting favorable docking scores, high ligand affinity, and low binding free energies, as determined by Glide docking, were subsequently subjected

to pharmacokinetic evaluation using ADME predictions through the QikProp module of the Schrödinger suite.[17]

RESULTS

HR-LCMS

The metabolites that were identified in the methanolic fraction of *A. baccifera* were subjected to LC-HRMS analysis. The extracted ion chromatograms obtained in both the positive and negative electrospray ionization modes are shown in Figure 1. The addition of formic acid to the mobile phase significantly enhanced the peak resolution and ionization efficiency. Due to the structural similarity among certain metabolites, some chromatographic peaks may represent co-eluting compounds with identical retention times. Following chromatographic separation, the metabolites were subjected to high-resolution tandem mass spectrometry using an Agilent Q-TOF system to obtain their characteristic fragment ion patterns, which are summarized in Table S1. Detection was performed in both positive and negative ionization modes to ensure comprehensive coverage of the metabolites.[18]

LC-HRMS profiling of the extract revealed a chemically rich composition encompassing monoterpenes, sesquiterpenes, phenolics, phenylpropanoids, coumarins, alkaloids, lignans, stilbenes, flavonoids, urolithins, and multiple glycosylated metabolites. The monoterpene and oxygenated monoterpenoid fractions included camphene (Mass 136.1255; $C_{10}H_{16}$), (+)-fenchone (Mass 152.120; $C_{10}H_{1616}O$), (–)-borneol (Mass 154.1359; $C_{10}H_{18}O$), (–)-menthol (Mass 156.1519; $C_{10}H_{20}O$), and oxidized derivatives such as 10-Hydroxyfenchone (Mass 168.1148; $C_{10}H_{16}O_2$), 2-exo-Hydroxy-1,4-cineol (Mass 170.131; $C_{10}H_{18}O_2$), and 1,4-cineol-9-carboxylic acid (Mass 184.1103; $C_{10}H_{16}O_3$). Sesquiterpenes and their oxygenated analogues include Vitispirane (Mass 192.1515; $C_{13}H_{20}O$), Patchoulen-β (Mass 190.1722; $C_{14}H_{22}$), Feniculin (Mass 202.1365; $C_{14}H_{18}O$), Nootkatone (Mass 218.1681; $C_{15}H_{22}O$), 14-Hydroxycaryophyllene-5,6-oxide (Mass

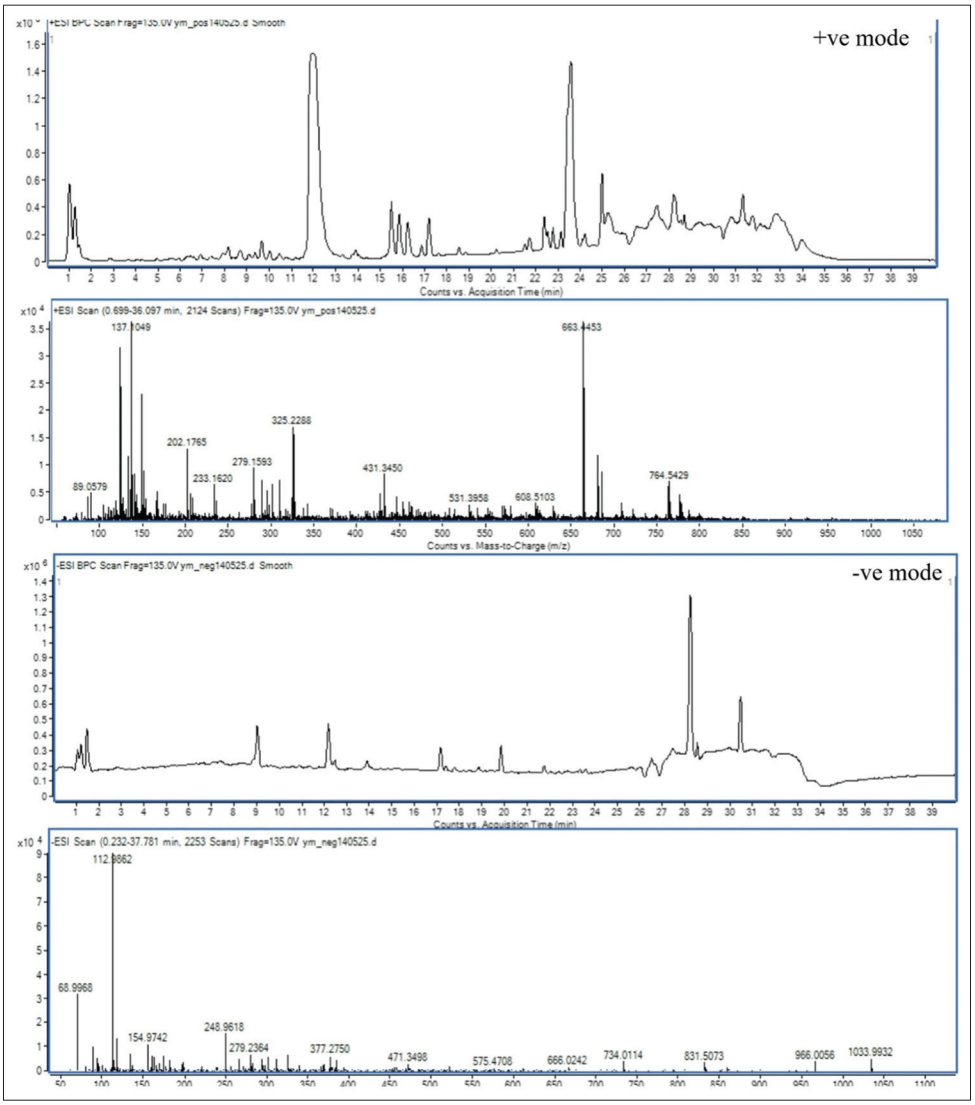

Figure 1: Chromatograms and mass spectra of the ethanolic extract of *Ammannia baccifera* in both positive and negative mode

236.1769; $C_{15}H_{24}O_2$), and Nootkatone-13,14-diol (Mass 252.1738; $C_{15}H_{24}O_3$). Higher terpenoids and lipophilic sterols were also identified, including Betulinic acid (Mass 456.3624; $C_{30}H_{48}O_3$), Diosgenin (Mass 414.3137; $C_{27}H_{42}O_3$), Sarsasapogenin (Mass 416.3301; $C_{27}H_{44}O_3$), and γ-Tocopherol (Mass 416.3657; $C_{28}H_{48}O_2$). A broad spectrum of phenolics and phenolic acids was observed, including Catechol (Mass 110.0366; $C_6H_6O_2$), 3-Methylcatechol (Mass 124.0524; $C_7H_8O_2$), 3′-Hydroxytyrosol (Mass 154.0623; $C_8H_{10}O_3$), Hydroxycaffeic acid (Mass 196.0375; $C_9H_8O_5$), 3,5-Dihydroxycinnamic acid (Mass 180.0424; $C_9H_8O_4$), Caffeoyl-o-quinone (Mass 178.0264; $C_9H_6O_4$), 3-O-Methylgallic acid (Mass 184.037; $C_8H_8O_5$), Maclurin (Mass 262.0488; $C_{13}H_{10}O_6$), Ellagic acid (Mass 302.0068; $C_{14}H_6O_8$), and the high-mass tannin Tellimagrandin I (Mass 786.0934; $C_{34}H_{26}O_{22}$). Phenylpropanoids and aromatic ethers included anethole (Mass 148.0881; $C_{11}H_{12}O$), Carvacrol (Mass 150.1039; $C_{11}H_{14}O$), 4-Ethylguaiacol (Mass 152.0837; $C_9H_{12}O_2$), 2-Methoxy-5-propenylphenol (Mass 164.0843; $C_{11}H_{12}O_2$), and Curcumene-α (Mass 202.1715; $C_{15}H_{22}$). Organosulfur phenylpropanoids were also detected, including erucin (Mass 161.034; $C_6H_{11}NS_2$), allicin (Mass 162.0178; $C_6H_{10}OS_2$), and Z-ajoene (Mass 234.0206; $C_9H_{14}OS_3$). The extract contained several coumarins and benzopyrones, including Umbelliferone (Mass 162.0324; $C_9H_6O_3$), Herniarin (Mass 176.0481; $C_{10}H_8O_3$), Scoparone (Mass 206.0586; $C_{11}H_{10}O_4$), and Lettucenin A (Mass 240.0794; $C_{15}H_{12}O_3$). Alkaloids were represented by Calystegin A3 (Mass 159.089; $C_7H_{13}NO_3$) and lupinine (Mass 169.1466; $C_{10}H_{19}NO$), alongside nitrogen–oxygen conjugates such as N-(2-Furoyl)glycine (Mass 169.0379; $C_7H_7NO_4$) and ethanolamine-betaxanthin (Mass 254.0914; $C_{11}H_{14}N_2O_5$). Lignans, stilbenes, and urolithins included Dihydro-resveratrol (Mass 230.0951; $C_{14}H_{14}O_3$), 3,4′-Dihydroxy-trans-stilbene (Mass 212.0839; $C_{14}H_{12}O_2$), Isourolithin B (Mass 212.0473; $C_{13}H_8O_3$), Secoisolariciresinol (Mass 362.1733; $C_{20}H_{26}O_6$), 3,10-Dihydroxy urolithin (Mass 228.0423), and 3,4,10-Trihydroxy urolithin (Mass 244.038). A rich diversity of flavonoids, isoflavones, and their glycosides was detected, including Coumestrol (Mass 268.0381), 2′-Hydroxydaidzein (Mass 270.0533), 6-Hydroxydihydrodaidzein (Mass 272.0688), 3′-Hydroxy-genistein (Mass 286.0491), Irilone (Mass 298.0485), Tetramethylscutellarein (Mass 342.1089), Kaempferol 3,7-O-diglucoside (Mass 610.1562), Cyanidin 3-O-sambubioside (Mass 581.1497), and Pelargonidin 3-O-sambubioside (Mass 565.1541). Additional sulfated and glycosylated metabolites included cis-resveratrol 3-sulfate (Mass 308.0341), Tectorigenin 7-sulfate (Mass 380.020), and piceatannol sulfate (Mass 324.0305). The polar methanolic fraction was further characteristic by the presence of carbohydrates and high molecular weight flavonoid conjugate compounds namely , arbutin (m/z 272.0903; $C_{12}H_{16}O_7$) and chrysoeriol 7-O-(6″-malonyl apiosyl-glucoside) (m/z 680.1607), indicating the occurrence of glycosylated phenolic metabolites with relatively high-molecular-masses.

In vitro antioxidant potential of *Ammannia baccifera*

The ethanolic extract of *A. baccifera* demonstrated significant radical scavenging activity against DPPH radicals across a range of concentrations (20, 40, 60, 80, and 100 µg/mL), with an IC_{50} of 56.68 µg/mL, compared to 47.34 µg/mL for ascorbic acid. The most pronounced radical scavenging effect was observed at 100 µg/mL compared to that of the control [Figure 2]. Additionally, the antioxidant potential of *A. baccifera* was assessed *in vitro* using the $ABTS^+$ scavenging and ferric ion ($Fe3^+$)-reducing power assays, with ascorbic acid as a standard. *A. baccifera* exhibited a notable antioxidant effect by scavenging $ABTS^+$ ions, achieving an IC_{50} value of 59.46 µg/mL, and effectively reduced $Fe3^+$ ions to ferrous ions with an IC_{50} of 68.78 µg/mL, while ascorbic acid had an IC_{50} of 48.09 µg/mL [Figure 2]. This antioxidant potential suggests that the phytochemicals in *A. baccifera* may contribute to its activity.[19]

Molecular docking studies

The molecular docking assay conducted on the 4L7D protein showed several phytochemicals having promising binding affinity and energy of interaction are shown in Table S2. In the compounds assessed during the study, the isoflavonoids and flavonoid glycosides showed the highest binding capacity, which was confirmed through Orobol (−7.071 kcal/moL), (3R)-4′-Methoxy-2′,3,7-trihydroxyisoflavanone (−7.024 kcal/moL), 6,7,4′-Trihydroxyisoflavanone (−6.713 kcal/moL), Cyanidin 3-O-sambubioside (−6.644 kcal/moL), Irilone

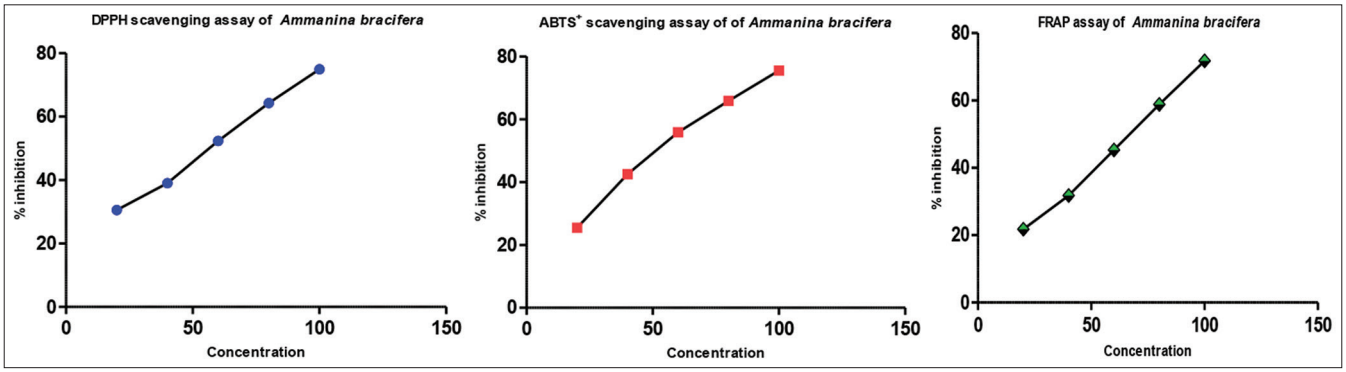

Figure 2: *In vitro* antioxidant potential of the ethanolic extract of *Ammannia baccifera*

(−6.503 kcal/moL), and Astilbin (−6.175 kcal/moL). The binding of the above compounds is further supported by their high Glide energy of −41.9 to −56.2 kcal/mol, which is indicative of extensive hydrogen bonding. Flavonoids, coumarins, lignans, and alkaloids such as Coumestrol, Tetramethylscutellarein, Umbelliferone, Scoparone, Secoisolariciresinol, Calystegin A3, and Lupinine demonstrated moderate binding affinities with docking scores varying between –4.5 and –6.3 kcal/mol. However, small phenolics, monoterpenes, and sulfur-containing compounds, such as Camphene, Menthol, Fenchone, Erucin, and Z-Ajoene, showed poor affinity towards the 4L7D protein, attributed to the low aromaticity and low hydrogen bonding capability. In general, isoflavonoids, anthocyanins, and flavonoid glycosides have better binding capabilities to the protein 4L7D since they contain many hydroxyl groups, aromatic rings, and flexible structures, allowing them to form strong hydrogen.

Molecular dynamics

Protein-ligand interaction stability was examined using 200 ns MD simulation results with root mean square deviation (RMSD), root mean square fluctuation (RMSF), and protein-ligand interaction calculations. During the MD simulations, the protein backbone RMSD remained very stable with values of RMSD ranging from 0.9 to 1.3 Å following the equilibrium stage, indicating that there were no structural changes in the protein due to binding with the ligand. The RMSD for the ligand also increased initially during the first 50 ns as the ligand adapted itself to its environment, after which RMSD values were stable at levels of 0.9 to 1.2 Å until the end of the simulation, showing no dissociation from the active site. The RMSF indicated that the protein had a rigid structure, with residues having low RMSF values (0.3–0.7 Å), except for some regions where there were moderate values [Figure 3a and b]. A noticeable high RMSF value around residue 50 could indicate loop flexibility associated with ligand binding.

The protein-ligand interaction study showed the presence of a stable and diverse protein-ligand interaction network, where ASN186 provided a stable hydrogen bond and water bridge network for more than 30% of the total simulation time. Stabilization was also observed via the interactions of residues like THR41, ARG35, SER32, VAL164, TYR51, and GLN168 with hydrogen bonds and hydrophobic interactions, whereas ASP129, GLU126, HIS102, TRP74, and LEU262 were involved in temporary protein-ligand interactions [Figure 3c and d]. Overall, the analyses of RMSD, RMSF, and protein-ligand interactions clearly indicated that the ligand was stably associated with the binding site due to hydrogen bonds, hydrophobic, and water bridges.

ADMET analysis of phytochemical compounds identified from ethanolic extract of *A. baccifera*

Table S3 provides information on the physicochemical properties of the investigated compounds, including molecular weight (MW), hydrogen bond acceptors (HBA), hydrogen bond donors (HBD), and adherence to Lipinski's rule of five and three. Most compounds had MWs below the recommended cut-off value (MW<500 Da), demonstrating promising drug-like properties. For example, molecules such as (−)-menthol (156.267 Da), (+)-fenchone (152.236 Da), and anethole (148.204 Da) had optimal MW values, implying

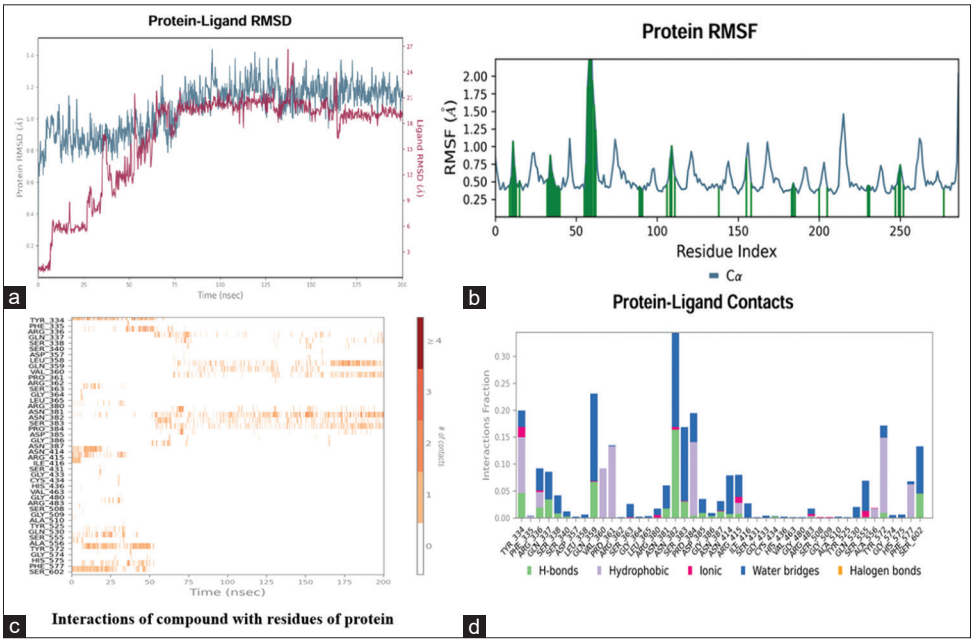

Figure 3: (a) Root mean square deviation of the stands for the HER2 Kinase Domain (3RCD) protein backbone in complex with compound 1a for 200 ns molecular dynamics simulation time (b) root mean square fluctuation variations of protein (c) the interactions of compound with residues of protein (d) Protein-ligand contacts of ligand-protein complex

high permeability and absorption potential. Conversely, bulky molecules such as tellimagrandin I (786.566 Da) and kaempferol-3,7-O-diglucoside (1332 Da) exceeded this value, reducing their oral availability.[20]

Hydrogen bonding interactions further validated the drug-likeness of the tested compounds. The majority of the molecules had acceptable numbers of HBAs (<10) and donors (<5) required for membrane permeability. However, polar molecules such as tellimagrandin I (HBA: 20.7, HBD: 13) and astilbin (HBA: 13.25, HBD: 6) had unacceptable HBA/HBD ratios, implying poor permeability. In addition, glycosides and glucuronides exhibit increased hydrogen bonding interactions, which may impede passive diffusion. According to Lipinski's rule of five, most drugs were observed to have little or no violations, signifying good oral drug-like properties. Drugs with one violation included (+)-gamma-tocopherol, betulinic acid, Diosgenin, and Sarsasapogenin, which were probably due to their higher MWs and/or greater lipophilicity. In contrast, complex flavonoid glycosides, including chrysoeriol analogs and Tellimagrandin I, had two or more violations, implying poor drug-like properties.

Table S4 gives parameters for ADMET, including human oral absorption, plasma protein binding (QPlogKhsa), Caco-2 permeability (QPPCaco), inhibition potential of HERG (QPlogHERG), permeability of the blood-brain barrier (BBB) (QPlogBB), and Madin-Darby canine kidney cell permeability (QPPMDCK). Most compounds had a high level of predicted human oral absorption, and some compounds, including (−)-menthol, (+)-Fenchone, Anethole, Carvacrol, and beta-damascenone, had an absorption rate of 100%, indicating high oral bioavailability. Conversely, Chrysoeriol glycoside and Tellimagrandin I had the lowest percentage of human oral absorption (0%) because of their high polarity and MW.

Caco-2 permeability results indicated that smaller and less polar compounds diffused easily across the membrane, and some compounds with a QPPCaco of approximately 9906, including Anethole and Camphene, had high intestinal permeability, whereas highly polar compounds, such as flavonoid glycosides and sulfated derivatives, had low permeability of <10. Similar results were obtained for MDCK permeability. The QPlogHERG values suggest that most of the compounds are safe in terms of the toxicity associated with the inhibition of the HERG channel; however, compounds such as Carvedilol (−8.125) and Tellimagrandin I (−6.101) had low values, indicating a risk of cardiotoxicity. The BBB (QPlogBB) values indicated that most compounds lacked central nervous system penetration, which is beneficial for drugs acting on other tissues. In contrast, smaller and lipophilic compounds exhibit a higher degree of BBB permeability. From the overall ADMET profile analysis, we concluded that smaller and lipophilic compounds possess a better pharmacokinetic profile characterized by good absorption and permeation; conversely, larger, more polar, and glycosylated compounds are poor absorbers and less bioavailable.

CONCLUSION

The present study suggests an organized assessment of the protective efficacy of *A. baccifera* through phytochemical profiling, computational approaches, integrated metabolomics, and *in vitro* studies. UHPLC-HRMS analysis of *A. baccifera* revealed a diverse profile of polyphenols, flavonoids, and terpenoid derivatives. Substantial antioxidant activity was observed with *A. baccifera* extract, validating its potential free radical scavenging activity through $ABTS^{+}$ and FRAP ion quenching. Using the computational technique of molecular docking, several active ingredients were found to bind effectively with the Keap1 protein, especially those residues that are involved in Nrf2/HO-1 pathway regulation. The integrity of the ligands bound to the receptors through molecular dynamics and ADMET predictions indicated the excellent drug-like and pharmacokinetic properties of the selected compounds, which effectively modulated the Keap/Nrf2/HO-1 signaling pathway to elicit the antioxidant effect. In conclusion, the current study demonstrates that *A. baccifera* is a valuable natural source of bioactive compounds that can regulate oxidative stress signaling pathways, particularly the Keap1-Nrf2 pathway. Further studies are warranted to establish the modulation of the Keap1-Nrf2 pathway in cell lines and experimental animal models at the molecular level.

REFERENCES

1. Martin SS, Aday AW, Almarzooq ZI, Anderson CA, Arora P, Avery CL, *et al*. 2024 heart disease and stroke statistics: A report of US and global data from the American heart association. Circulation 2024;149:e347-913.
2. Hausenloy DJ, Yellon DM. Myocardial ischemia-reperfusion injury: A neglected therapeutic target. J Clin Invest 2013;123:92-100.
3. Perrelli MG, Pagliaro P, Penna C. Ischemia/reperfusion injury and cardioprotective mechanisms: Role of mitochondria and reactive oxygen species. World J Cardiol 2011;3:186-200.
4. Wang CZ, Mehendale SR, Yuan CS. Commonly used antioxidant botanicals: Active constituents and their potential role in cardiovascular illness. Am J Chin Med 2007;35:543-58.
5. Zern TL, Fernandez ML. Cardioprotective effects of dietary polyphenols. J Nutr 2005;135:2291-4.
6. Oyaizu M. Studies on products of browning reactions: Antioxidative activities of product of browning reaction prepared from glucosamine. Jpn J Nutr Diet 1986;44:307-15.
7. Graham SA, Timmermann BN, Mabry TJ. Flavonoid glycosides in *Ammannia coccinea* (Lythraceae). J Nat Prod 1980;43:644-5.

8. Vinod A, Chandra Mouli H, Jana A, Peraman R. Unlocking therapeutic potential: Exploring indole scaffolds and their structural insights as pharmacophores in designing anti-breast cancer agents. Med Chem Res 2024;33:1100-32.
9. Myrsing E, Vinod A, Mouli HC, Ravichandiran V, Jana A. Utilizing graphene oxide (GO) catalysed cascade in the synthesis of tetracyclic pyrano [3, 4-b] indole derivatives. Asian J Org Chem 2023;12:e202300126.
10. Harini D, Mouli HM, Raman PK, Singh N, Shreya S, Khemchandani R, *et al*. Phytoconstituents of *Gmelina arborea* as potential breast cancer inhibitors: LC-MS/MS, docking, MD simulations, and *in vitro* evaluation. Chem Biodivers 2026;23:e01930.
11. Sawi SE, El-Feky AM, El-Sayed MI, El-Sayed AF. Therapeutic potential of isolated flavonoids from anise and coriander aerial parts in antimicrobial efficacy, molecular docking, ADMET, and dynamic simulations. Sci Rep 2025;15:26485.
12. Singleton VL, Orthofer R, Lamuela-Raventós RM. Analysis of total phenols and other oxidation substrates and antioxidants by means of folin-ciocalteu reagent. Methods Enzymol 1999;299:152-78.
13. Mouli HC, Harini D, Shaikh N, Khemchandani R, Shreya S, Jana A, *et al*. *In silico* characterization of indole-substituted densely functionalized pyrrole against breast cancer: Integrating DFT, molecular docking, MD simulations, and ADME analysis. J Mol Struct 2025;1328:141375.
14. Hussain MZ, Myrsing E, Mouli HC, Dey K, Khajuria S, Paul AK, *et al*. Exploring anticancer potential of furopyrano[3,4-b]indole via graphene oxide-catalyzed aqueous synthesis. ChemistrySelect 2024;9:e202404316.
15. Ivánczi M, Balogh B, Kis L, Mándity I. Molecular dynamics simulations of drug-conjugated cell-penetrating peptides. Pharmaceuticals (Basel) 2023;16:1251.
16. Moulishankar A, Lakshmanan K. Data on molecular docking of naturally occurring flavonoids with biologically important targets. Data Brief 2020;29:105243.
17. Guan L, Yang H, Cai Y, Sun L, Di P, Li W, *et al*. ADMET - score - a comprehensive scoring function for evaluation of chemical drug-likeness. Medchemcomm 2018;10:148-57.
18. Myrsing E, Mouli HM, Nikhil P, Deepali, Sahu A, Jana A, *et al*. Protein profiling uncovers IGF-1R inhibition potential of 3-(2-furoyl)-indole Scaffolds in hepatocellular carcinoma. Future Med Chem 2025;17:513-28.
19. Loganayaki N, Siddhuraju P, Manian S. Antioxidant, anti-inflammatory and anti-nociceptive effects of *Ammannia baccifera* L. (Lythracceae), a folklore medicinal plant. J Ethnopharmacol 2012;140:230-3.
20. Jamrozik E, Smieja M, Podlewska S. ADMET-PrInt: Evaluation of ADMET properties: Prediction and interpretation. J Chem Inf Model 2024;64:1425-32.

Source of Support: Nil. **Conflicts of Interest:** None declared.